Singlet exciton transport in substitutionally disordered naphthalene crystals: Percolation and generalized diffusion[a)]

Stuart T. Gentry and Raoul Kopelman

Department of Chemistry, The University of Michigan, Ann Arbor, Michigan 48109
(Received 30 June 1982; accepted 31 August 1982)

Experimental data is presented for singlet exciton transport in a ternary naphthalene system ($C_{10}H_8/C_{10}D_8$/BMN). The trapping probability varies with guest concentration and with temperature. The data at 4.2 K are consistent with a generalized diffusion treatment such as that proposed by Gochanour, Andersen, and Fayer. The 1.8 K data conform to a quasistatic percolation model. The supertrap induced energy funnels which might affect this energy transport are limited to nearest neighbors. The BMN fluorescence spectra are affected by exciton–phonon interactions similar to Herzberg–Teller coupling.

I. INTRODUCTION

Energy transport in molecular crystals has been studied extensively for over 30 years.[1–3] In spite of the large amount of work done in this field, there are still basic questions of interest regarding the dynamics of excitons. Within the past four years a number of researchers have tackled theoretically the generalized diffusion of excitons in a mixed molecular crystal.[4–9] To help fill the widening gap between these increasingly sophisticated theoretical models and the available experimental information we have extended previous studies on the model system of substitutionally disordered isotopic mixed naphthalene crystals.[2,3]

It is necessary to define several terms since there is an abundance of differing nomenclature in the literature. For our ternary crystal system we will refer to perdeuteronaphthalene, naphthalene, and betamethylnaphthalene as host, guest, and supertrap, respectively. The supertrap concentration is in the dilute limit so that we can assume that any supertrap emission is the result of energy transport from the guest manifold. A useful parameter for measuring the extent of energy transport among the guest sites is the trapping probability P. P is defined as the number of excitons residing on supertrap sites divided by the total number of excitons in the system. This parameter is model independent. For steady state experiments it is also time independent.

We have chosen to discuss our results in light of three different theoretical models. One is percolation. The other two are generalized diffusion models (hereafter referred to simply as diffusion). We found that the energy transport in naphthalene at a temperature of 4.2 K is in good agreement with diffusion. At 1.8 K the data are consistent with a quasistatic percolation model. The diffusion model (assuming octupole–octupole transfer) breaks down at the lower temperature due to the energetic differences between neighboring naphthalene clusters. It may also be that it is no longer appropriate to treat the excitons as strictly localized states. Finally, we found that there is no significant enhancement in the trapping probability caused by supertrap induced energy funnels.

In Sec. II we review and compare the different models used to predict exciton transport phenomena. Section IV describes the experimental results while Sec. V discusses the results in light of the theoretical models. Sec. VI deals with the related question of energy funnels.

II. THEORETICAL MODELS

A. Percolation

Broadbent and Hammersley[10] introduced the percolation problem in 1957. They describe the connectivity of conducting sites in a conductor/insulator random binary lattice. Conducting networks, or clusters, are defined as contiguous sequences of conductor sites. The most striking feature of site percolation is that as the composition of the binary lattice is varied, a critical concentration is reached. Around this threshold concentration the size of the largest cluster in the lattice rapidly increases until it spans the lattice.

Kopelman and co-workers have suggested that site percolation can explain exciton transport phenomena in mixed crystals and have applied their theory to a number of naphthalene crystal systems.[2,3] Colson *et al.* have applied percolation to a benzene crystal system.[11] It is a well accepted fact that clusters play a major spectroscopic role in isotopic mixed crystals. At low guest concentrations the emission resulting from monomer, dimer, and trimer clusters is easily resolvable.[12] Given that an exciton may be described as a localized or quasilocalized state, it is straightforward to apply the cluster formulation to the percolation model.

Static percolation requires two assumptions. The first is that there is an effective cutoff for the allowable interaction distance between two guest sites, e.g., only nearest, next-nearest, and third-nearest neighbor interactions are allowed. (The specific cutoff distance is defined by the lifetime of the exciton.) The second assumption is that the dynamics within a cluster can be ignored. In a ternary crystal this implies that if an exciton lands on a cluster containing a supertrap, then it will find that supertrap within the time scale of the experiment.

[a)]Supported by NSF Grant No. DMR 8000679.

 0021-9606/83/010373-10$02.10

There are several variations to the static percolation model. Dynamic percolation permits the interaction distance to increase with time.[13] This model has been used to interpret naphthalene triplet experiments where the exciton lives long enough to undergo super-exchange tunneling between clusters. Quasistatic percolation has been suggested to explain singlet data in the case of dilute supertrap concentrations.[14] For the latter condition the exciton may not live long enough to find the supertrap sites within the largest clusters. This influence of finite lifetime has been included in the percolation model[2,14,15] via simulations of random and correlated walks on the maxiclusters. In the limit of supertransfer, i.e., visitation of *all* supertrap sites within the exciton lifetime, the random walk results reduce mathematically to the static percolation limit.

For the current experimental study the most important prediction of the static percolation model is that[15]

$$P = \sum_m [1-(1-m/G)^Z] i_m m/G \ , \tag{1}$$

where i_m is the frequency of clusters of size m and G and Z are the number of guest and supertrap sites, respectively. Another feature of percolation is that P is well defined by critical exponent behavior at concentrations well above and well below the critical concentration as well as right at the critical concentration.[3]

$$P \propto \left| \frac{C}{C_c} - 1 \right|^{-\gamma} , \quad C \ll C_c; \ S \ll 1 , \tag{2}$$

$$P \propto (S)^{1/\delta} , \quad C = C_c; \ S \ll 1 , \tag{3}$$

$$P \propto \left| \frac{C}{C_c} - 1 \right|^{\beta} , \quad C \gg C_c; \ S \ll 1 , \tag{4}$$

where S is the relative supertrap concentration ($S = Z/G$) and $\delta = 1 + (\gamma/\beta)$. These critical exponents provide a measure of the dimensionality of the exciton transport. For two-dimensional transport we expect $\gamma = 2.39$ and $\beta = 0.14$, while for three-dimensional transport the prediction is that $\gamma = 1.78$ and $\beta = 0.4$.[3] Furthermore, fractional dimensionality may also be simulated.[15,16] This is relevant when the transport interactions are mainly two dimensional, but with transfer in the third direction not completely negligible. One final ramification of the critical exponent behavior of percolation is that a plot of P vs reduced concentration C/C_c should be independent of the interaction distance used to define the clusters.[3] We note that actual random walk simulations[2] indeed give sharply rising P curves that closely resemble the shape of the static percolation curves. Consequently we derive the quasistatic percolation curve, for the reduced concentration plot, from the easily calculable static curve, without recourse to model dependent random walk simulations.

The algorithm for calculating the static percolation P is to construct a random binary host/guest lattice with a specified guest concentration. Using the cluster multiple labeling technique[29] one can determine the number of clusters of size m found in this lattice. After finding these i_m values, averaged over several lattices, it is straightforward to apply the results to Eq. (1). Notice that the supertrap concentration (implicitly given by Z) only affects the trapping probability, not the cluster frequency i_m.

B. Diffusion models

Percolation requires the use of computer simulations to study exciton transport phenomena. An alternative method of studying exciton transport is to analytically predict the dynamic behavior of excitons in disordered media. Two approaches to the analytic problem are the use of a master equation and the use of continuous time random walk equations.[4] In the interest of brevity we have chosen to apply our results only to the work done by Loring and Fayer,[5] based on the theory of Gochanour, Andersen, and Fayer (GAF)[6] as well as to the Blumen and Silbey result.[7] In both cases, multipole transfer between two sites separated by a distance r_{jk} is treated by using the orientationally averaged Förster transfer rate:

$$w_{jk} = \tau^{-1} (R_0/r_{jk})^n \ . \tag{5}$$

In the case of octupole–octupole interactions $n = 14$. R_0 can be thought of as the distance corresponding to a transfer time equal to the exciton natural lifetime. It is treated as an adjustable parameter. GAF assume the high temperature limit, i.e., $w_{jk} = w_{kj}$.

The Loring, Anderson, and Fayer (LAF) model,[6(b)] which is used by Loring and Fayer,[5] is an adaptation of the GAF model[6(a)] designed to account for exciton trapping as well as exciton transfer. The underlying approach in all of these papers is to find a Green function solution to a kinetic master equation. The GAF solution is similar to that suggested by Haan and Zwanzig.[8] Both models use a series expansion solution for $\hat{G}^m(\mathbf{k}, \epsilon)$, the Laplace–Fourier transform of the probability that the exciton is found at site r at time t, given that it was at the origin at $t = 0$. Haan and Zwanzig solve for $G^m(\mathbf{k}, \epsilon)$ in terms of an expansion in powers of guest concentration, i.e., solve $\hat{G}^m$ for a two particle system averaged over all configurations, then for a three particle system, etc. The strength of the GAF solution lies in two interrelated steps. By use of an elegant diagrammatic procedure, they are able to add a large number of interactions involving other particles to their two-body result as well as to their higher order results. Concomitant with this procedure is the requirement that the diagrammatic solutions obey a total probability normalization equation. The result is a self-consistent system of equations which in general yield significantly better results than the method suggested by Haan and Zwanzig.

Loring and Fayer[5] show that the LAF adaptation to the GAF model gives (for equal guest and supertrap lifetimes)

$$P = 1 - k_g \hat{G}^g(0, \epsilon = k_g) \ . \tag{6}$$

$\hat{G}^g(0, \epsilon)$ is the Laplace transform of the time dependent part of the systems Green function which gives the probability of finding an exciton somewhere within the guest manifold. k_g^{-1} is the guest lifetime.

$\hat{G}^g(0, \epsilon)$ is found by using the LAF diagrammatic equations for guest–guest transfer and guest–supertrap transfer. Loring and Fayer discuss several ramifica-

tions of their results. One is the well accepted fact that critical concentration behavior will not be seen if transfer is dominated by long range dipole–dipole interactions. They also show that in the case of no supertraps and dipole–dipole transfer, the exciton transport becomes diffusive in the long time limit as expected. Furthermore, for two- and three-dimensional transfer the diffusion coefficient is larger than the Einstein prediction made for guests distributed evenly over a superlattice.

Blumen and Silbey have presented an alternative to the more rigorous theories designed to predict exciton dynamics.[7] This model warrants being mentioned because of the ease involved in using it. They use simplified equations to calculate an average hopping time from a guest site and the probability that that hop will be to a supertrap site. These two expressions are used to develop an energy trapping rate constant K_{ET}. The steady state trapping probability is found by using K_{ET} in a set of kinetic equations. For multipole transfer with C_s/C_g = constant, they derive the expressions:

$$K_{ET}^{-1} = \text{constant}/[(C_s/C_g)\,C_g^r]\,, \tag{7}$$

$$P = 1/[1+(C_{1/2}/C)^r]\,, \tag{8}$$

where $C_{1/2}$ is defined to be the concentration that corresponds to $P = 0.50$. The exponent is given by the function $r = n/d$, which is dependent on the dimensionality d and the multipole transfer exponent n from Eq. (5).

C. Comparison of percolation and diffusion models

It is enlightening, with respect to the experimental results which follow in this paper, to compare several features of the percolation and diffusion approaches. One conclusion that can be drawn is that they are not in fundamental competition with one another. Both types of models are attempts to treat a very complicated kinetic problem, i.e., exciton transfer in randomly mixed molecular crystals. The difference between the two approaches lie in the approximations that are made to make the problem more tractable. In light of this statement, we should view percolation and diffusion solutions as offsetting, or complementing, one another.

One of the principal assumptions made in the static percolation model is that long range interactions can be ignored for sites separated by more than a given interaction distance. A major assumption made in the GAF model is that long range interactions are allowed, with the rate of transfer from one guest site to a second guest site equal to that of the reverse transfer step $w_{jk} = w_{kj}$. Monberg and Kopelman[17] point out that the latter statement is not a valid assumption for singlet naphthalene excitons at low temperatures. Irrespective of whether clusters dominate exciton transport, they will have a large effect on the exciton energetics.[12] A weighted average of the energy differential between guest clusters (δ) for a $C_g \simeq 0.30$ crystal gives $\delta \simeq 5$ cm^{-1}.[17] This fact has been used to justify limiting the energy transfer to nearest neighbors when explaining experimental data taken at liquid helium temperatures.

It is possible to compare transfer times between two resonant guest sites and between two nonresonant sites located on different clusters. The nearest neighbor resonant hopping time is on the order of 1 ps.[18] Conversely, the relaxation time from the upper to the lower dimer states of a $C_{10}H_8$ out-of-plane translationally equivalent pair in $C_{10}D_8$ is 50 ps.[19] The two dimer states are separated by 17 cm^{-1}.[19] If we assume that this relaxation time is limited by the acoustic phonon density of states, then other nonresonant exciton dynamic processes will be similarly affected. Therefore, transfer from one cluster to a cluster 1–5 cm^{-1} lower in energy must take longer than 50 ps. In addition, at a temperature of 1.8 K transfer to a cluster higher in energy will have to take one to two orders of magnitude longer than the 50 ps forward transfer, assuming detailed balancing. The resulting picture is one of fast transfer within a cluster, slow transfer to lower energy clusters and very slow transfer to higher lying clusters. An exciton can cascade down to lower energy clusters, but it will soon reach the lowest lying available cluster. All subsequent transfer is effectively limited to within that cluster.

The second important comparison to be made between the percolation and diffusion models is that the former ignores the dynamics of an exciton within a cluster while the latter explicitly considers the motion of a localized exciton. Excitons by their very nature are dynamic entities. Consequently, percolation should not be mistaken for being more than just a phenomenological model. Ignoring the exact behavior of the exciton within a cluster may be a limitation of percolation, but it can also be an asset. The model holds whether the exciton is strictly localized or whether it is partially coherent, just as long as it is localized with respect to the cluster boundaries. Coherence may have a large effect on the GAF model which is formulated on the premise of localized excitons.

Finally, percolation explicitly considers the discrete lattice. Both the Loring and Fayer model and the Blumen and Silbey model are solved by replacing the lattice with the continuum limit. Blumen and Manz' show that this is not a very good approximation for guest concentrations in the range of 0.5 to 1.0 mole fraction. In this region the discrete nature of the nearest, next-nearest and third-nearest neighbor distances becomes important.

III. EXPERIMENTAL

The crystals used in this study consisted of perprotonaphthalene ($C_{10}H_8$) and perdeuteronaphthalene ($C_{10}D_8$) taken from material which had been potassium fused and zone refined. Zone refined betamethylnaphthalene (BMN) was added in sufficient amount so as to give the crystals a relatively constant BMN: $C_{10}H_8$ mole ratio (C_s/C_g). The BMN concentration of each crystal was checked with optical absorption at 1.8 K. Any crystal with a supertrap: guest mole ratio outside of the range $0.6\times10^{-3} \le C_s/C_g \le 1.4\times10^{-3}$ was discarded. The crystals were grown using a modified Bridgeman technique and annealed for at least 48 h. Cleaved crystals less than 1 mm thick were mounted in a strain-free holder and immersed in liquid helium.

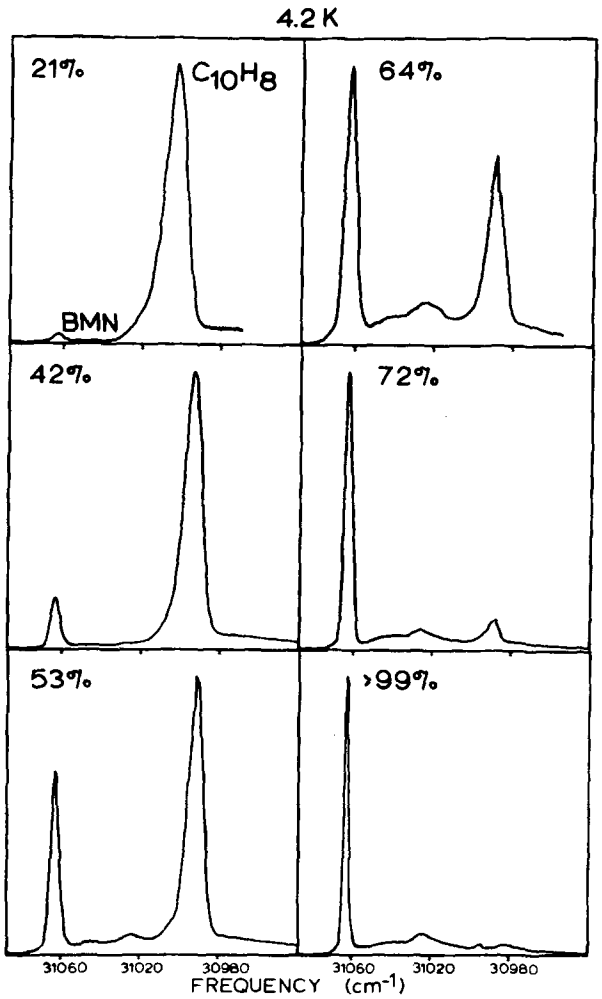

FIG. 1. Guest and supertrap fluorescence spectra for the ternary crystal system: $C_{10}D_8/C_{10}H_8/BMN$. The guest concentration was varied while maintaining a constant supertrap guest concentration ratio of 10^{-3}. This set of spectra was recorded at a temperature of 4.2 K. The BMN 0–0 zero-phonon peak is located at 31 061 ± 2 cm^{-1} for a 100% $C_{10}H_8/BMN$ crystal.

The crystals were optically excited by a 1600 W xenon lamp. For the fluorescence measurements, the radiation was filtered to allow through 2400–2900 Å light. The absorption studies used a bandpass of 2400–3700 Å. The signal detection system consisted of an ITT F-4013 cooled PMT, a Jarrell–Ash 1 m double monochromator and an SSR digital photon counter, interfaced to a PDP-11/03 microcomputer system. Data was transferred from the PDP-11 to an Amdahl 470V/8 computer to process the results. When it was necessary to calibrate the wavelength, a PAR chopper was used to alternate sampling between the optical signal from the crystal and an iron hollow cathode lamp.

IV. ENERGY TRANSPORT RESULTS

Figure 1 shows typical fluorescence spectra as a function of $C_{10}H_8$ concentration. The higher energy peak is due to the BMN 0–0 fluorescence. The broad feature with a maximum at about 31 015 cm^{-1} is a phonon sideband built on the BMN emission. The lower energy peak is the $C_{10}H_8$ 0–512 cm^{-1} fluorescence. Although the naphthalene 512 cm^{-1} peak occurs at lower energy than the BMN 0–0 peak, the naphthalene 0–0 peak is at a higher energy, ~31 541 cm^{-1}.

Our experimental definition for the trapping probability is

$$P = \frac{I_s}{I_s + \alpha I_g} , \tag{9}$$

where I_s is the intensity originating from the supertrap integrated over a limited spectral window, i.e., the integrated intensity of the BMN 0–0 band, and I_g is the guest intensity. α is an empirical factor which accounts for any difference between guest and supertrap in the proportionality constant which relates monitored emission intensity to the exciton concentration, i.e., differences in the quantum yield or spectral window factors. For this paper we used a value of $\alpha = 2.0$.[20] Examination of Fig. 1 reveals an additional problem when calculating P. There is considerable overlap between the BMN phonon sideband and the naphthalene emission. We separated the integrated emission values by measuring the BMN zero-phonon intensity and multiplying it by the ratio of zero phonon to total BMN intensity. This ratio is an optical Debye–Waller factor.

Previous papers treated the Debye–Waller factor as a constant, as is predicted by simple models. We have determined that this is not valid. There are two effects which influence the measured intensity ratio. One is the guest/host concentration dependence of the inhomogeneous supertrap linewidth. The line position for BMN-H_{10} shifts by 5 cm^{-1} from a $C_{10}H_8$ crystal to a $C_{10}D_8$ crystal. Clearly in our mixed crystals the BMN linewidth will be indicative of the statistical variation in environment around the supertrap sites. This line broadening causes a change in the overlap between the zero-phonon and phonon sideband emission. The second effect is the influence of the optical polarization on the Debye–Waller factor. A Franck–Condon model predicts that changing the polarization of the excitation or emission radiation can alter the overall intensity, but should not alter the *relative* amounts of zero-phonon and phonon sideband intensities. Experimentally we found that changing the polarization from ∥b to ∥a with respect to the crystallographic axes changed the Debye–Waller factor from 0.20 and 0.38. This variation in polarization also affected the sideband structure, e.g., in the 80–110 cm^{-1} region (Fig. 2). This dependence on the optical polarization is most likely due to a breakdown in the Condon approximation, due to an exciton–phonon interaction similar to Herzberg–Teller coupling.[21]

To determine P we made a large number of measurements on a 100% $C_{10}H_8$ crystal containing BMN while varying the optical polarization and resolution. The symmetrical nature of the observed fluorescence and BMN absorbance allow us to assign all of the emission from this crystal as originating from the supertraps, within an uncertainty of 1%. [We note that Loring and Fayer predict that the above 100% crystal, with 0.1% BMN, will have a value of P = 0.97 rather than 1.00 (cf. Sec. V of this paper).] We used the data to em-

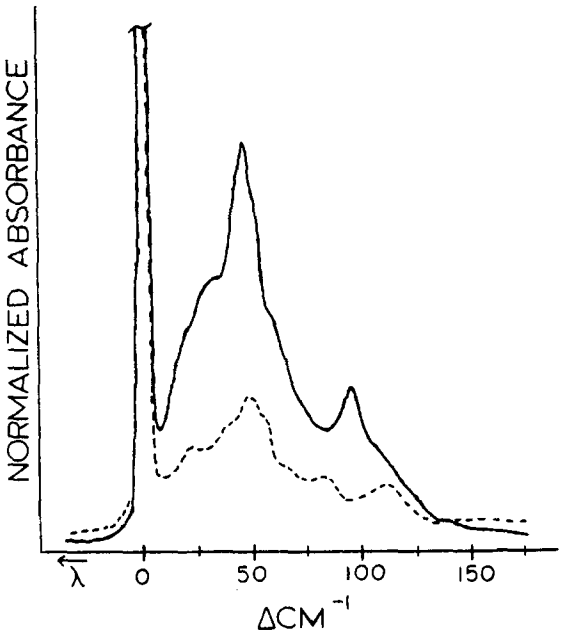

FIG. 2. Comparison of absorbance (optical density) plots of the BMN first singlet 0–0 transition in $C_{10}H_8$ for two different polarizations of the incident light. The absorbances have been normalized to the same zero-phonon peak height. In both cases the zero-phonon peak lies at 31 061 cm^{-1}. Solid line: ∥ b component; Dashed line: ∥ a component.

pirically obtain a functional relationship comparing the zero-phonon linewidth and the relative peak heights of the phonon and zero-phonon bands to the corresponding measured Debye–Waller factor. We subsequently applied this functional relationship which was derived from the case where there was no guest–supertrap emission overlap to the mixed crystals which did have overlap. An example of the importance of these corrections is the spectrum obtained at 4.2 K for our 72% crystal. Without the correction we calculated a trapping ratio P greater than 1.0. With the correction we found P = 0.71 which agrees with what a cursory visual estimation would give (cf. Fig. 1). A significant feature of this correction process was that after the correction equation was empirically obtained using a 100% $C_{10}H_8$/BMN crystal, its application to the isotopically mixed crystals had no adjustable parameters.

Figure 3 is a plot of P vs guest concentration for two temperatures. There are two notable features visible on this drawing. The first is the presence of critical behavior, i.e., a rapid increase in the trapping ratio over a narrow concentration range. The second notable feature is the temperature dependence of the critical concentration. This data is discussed in greater detail in Sec. V of this paper. The error bars on Fig. 3 are quite large due to the various data manipulation steps. Approximately half of the uncertainty, however, is due to the systematic uncertainty in the value of α used in Eq. (9) (cf. Ref. 20).

V. DISCUSSION OF ENERGY TRANSPORT RESULTS

Figures 3–5 compare the experimental trapping probabilities (for $C_s/C_g = 10^{-3}$) with the predictions made by the theories discussed in Sec. II. The percolation results [based on Eq. (9)] were taken from Monte Carlo simulations[16] on a 400×400 square lattice assuming only nearest-neighbor interactions and assuming that C_s/C_g is kept constant at 0.001. The Loring and Fayer curve was taken directly from Ref. 5. The curve is based on two-dimensional octupole–octupole transfer with a supertrap concentration of $C_s = 0.001$. They obtained the best fit, relative to the Monberg data,[20] using a value of $R_0 \simeq 8$ Å in Eq. (5). The Blumen and Silbey curve was calculated assuming two-dimensional octupole–octupole transfer with $C_s/C_g = 10^{-3}$. As pointed out by Loring and Fayer the GAF steady state result is very similar to that predicted by Blumen and Silbey. If we had calculated the Blumen and Silbey prediction keeping C_s fixed at 0.001, the result in Fig. 4 would be indistinguishable from the Loring and Fayer curve for $C_g/C_{1/2} > 1.0$. For $C_g/C_{1/2} < 1.0$ the curve would lie half way between the Loring and Fayer curve and the $C_s/C_g = 0.001$ Blumen and Silbey curve. In any case, the differences between the various generalized diffusion results are less than our experimental uncertainty. Figure 4 demonstrates that the largest qualitative difference between the percolation and diffusion model results is in the abrupt behavior of P near the critical threshold in the percolation case.

The experimental results suggest that the energy transport of singlet naphthalene excitons at 4.2 K is

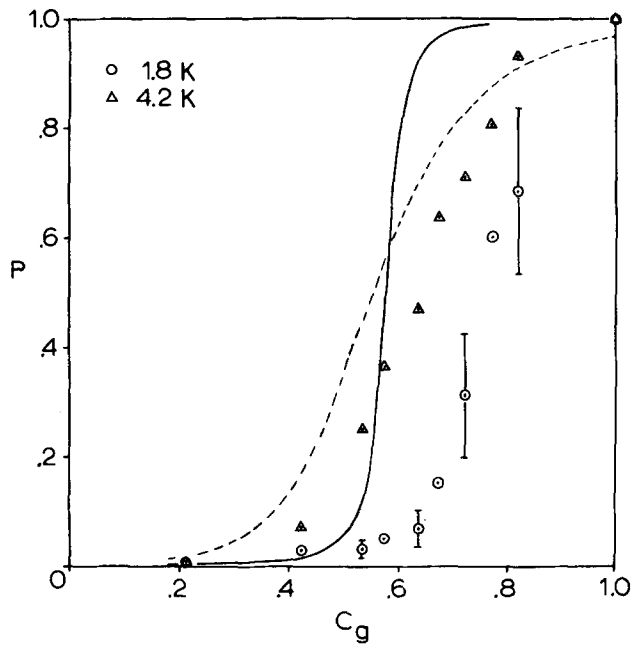

FIG. 3. Trapping probability vs guest concentration. Experimental points: Circles are 1.8 K data; Triangles are 4.2 K data. We have included several representative error bars. Theoretical: The solid line is the predicted curve using nearest-neighbor static percolation. The curve was calculated using Eq. (1), a supertrap : guest concentration ratio of 10^{-3} and computer simulations on a 400×400 square lattice. The dashed line is that calculated by Loring and Fayer (Ref. 5). They assumed a two-dimensional continuum and octupole–octupole interactions. The supertrap concentration was kept fixed at 10^{-3} mole fraction and they used a value of $R_0 \simeq 8$ Å.

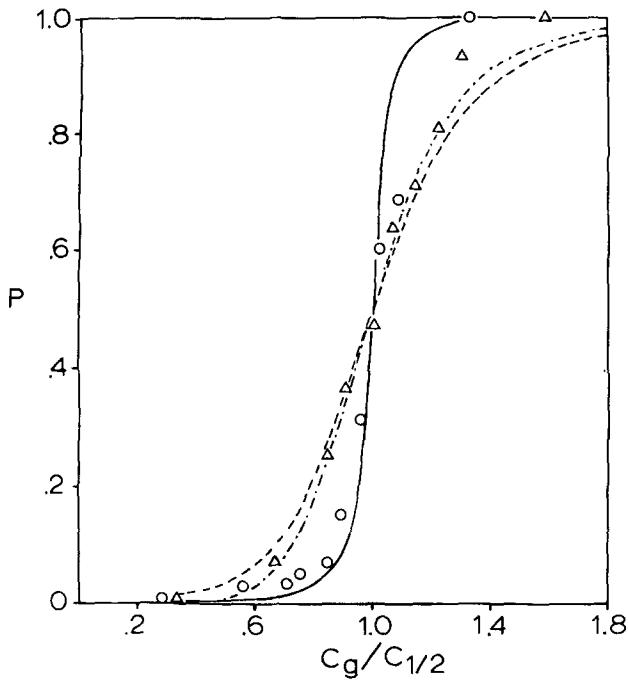

FIG. 4. Trapping probability vs reduced concentration. $C_{1/2}$ is defined as the concentration corresponding to $P=0.5$. Experimental: Circles are 1.8 K data; Triangles are 4.2 K data. Theoretical: The solid and dashed lines correspond to percolation and the Loring and Fayer calculation, respectively (cf. caption to Fig. 3). The dot–dashed line was calculated using the Blumen and Silbey model, Eq. (8). The Blumen and Silbey and the Loring and Fayer curves assume octupole–octupole transfer within a two-dimensional continuum. The experimental data, percolation, and Blumen and Silbey curves were calculated using $C_s/C_g=0.001$. The Loring and Fayer curve kept C_s constant at $C_s=0.001$. Changing the Loring and Fayer curve to account for a constant C_s/C_g ratio would only add a small correction. As a comparison, if the Blumen and Silbey equations were calculated using $C_s=0.001$ then the result would lie half way between the dot–dashed and the dashed lines for $C_g/C_{1/2}<1.0$. For $C_g/C_{1/2}>1.0$ the result is essentially identical to the Loring and Fayer curve.

best described by diffusion, assuming octupole–octupole transfer, while the 1.8 K results are more consistent with percolation. As discussed in Sec. II C, it is not surprising that the GAF model should break down at very low temperatures. The rate of transfer of an exciton from one guest site to a second guest site may not be the same in the forward direction as in the reverse direction owing to the energetic differences of the clusters. In addition at low temperatures excitons can no longer be treated as strictly localized states. Presumably raising the temperature from 1.8 to 4.2 K is enough to overcome these difficulties. Interpreting the 4.2 K results by using Loring and Fayer's equations is not without other problems. Using $R_0 \simeq 8$ Å, a nearest neighbor distance of $r_{nn}=5.1$ Å and the naphthalene lifetime of 120 ns gives a nearest neighbor transfer time of 200 ps when using Eq. (5). This hopping time is usually estimated to be on the order of 1 ps.[18] While it is true that there is some ambiguity in how this 1 ps transfer time should be interpreted with respect to the Loring and Fayer definition, it is not likely that this ambiguity will account for the two orders of magnitude discrepancy in hopping times. Loring and Fayer's slower transfer rate is rather likely to be a manifestation of their effective averaging over the slow back transfer between clusters and their use of a continuum model.

Given that percolation is no more than a phenomenological model, percolation and the 1.8 K data are in fairly good agreement. It is clear from Fig. 3 that static percolation cannot solely explain the data since the critical concentration is above that predicted by percolation, i.e., $C_{c,\mathrm{perc}}=0.593$. We can invoke quasistatic percolation however. This implies that even though an infinite cluster is formed at $C_g=0.593$, the exciton is unable to find a supertrap due to its lifetime constraint. One hypothesis to explain why the exciton does not necessarily have enough time to find a BMN molecule concerns the nature of the infinite cluster near the critical concentration. Large sections of the cluster consist of thin strands of guest sites connecting larger islands of guests. If the exciton is partially delocalized over several guest sites or if the random walk is partially coherent, then the exciton may be less likely to go down the thin connecting strands. Raising the guest concentration will reduce the number of thin strands relative to the number of islands until a threshold concentration is reached. This concentration is defined by the lifetime of the exciton. Clusters consisting of a large number of thin strands connecting various islands are described as *ramified*. Argyrakis and Kopelman have done work supporting the ideas discussed in this paragraph.[14] They found that they could obtain a good theoretical fit to their very dilute supertrap experimental data by adding one adjustable parameter to the quasistatic percolation model. The parameter was a random-walk coherence length. The effect of adding some correlation to the random walk was to inhibit energy transport except at the highest guest concentrations.

Assuming that ramified clusters and/or exciton coherence can be used to explain the high value of the critical concentration, we can use Figs. 4 and 5 to see whether the 1.8 K experimental results are consistent with quasistatic percolation. As mentioned in Sec. II A, percolation predicts that a plot of C/C_c should be independent of the interaction distance. Since $C_c \simeq C_{1/2}$, we should expect that the percolation curve and the 1.8 K experimental results should be superimposed on Fig. 4. Furthermore, we should be able to plot $\log|C/C_c-1|$ vs $\log P$ (as in Fig. 5) and get linear behavior away from the critical concentration. Using the 1.8 K data below the critical concentration gives an exponent of

$$\gamma=1.6\pm0.3,$$

as compared to the predicted two-dimensional value of $\gamma=2.39$. One note of caution regarding the preceding discussion is that we have assumed that the effect of quasistatic percolation on the scaling theory predictions is analogous to the effect of varying the interaction distance in static percolation. A second comment is that limiting the exciton transport to two dimensions is only a rough approximation for singlet naphthalene. Estimations of the out-of-plane interaction matrix element

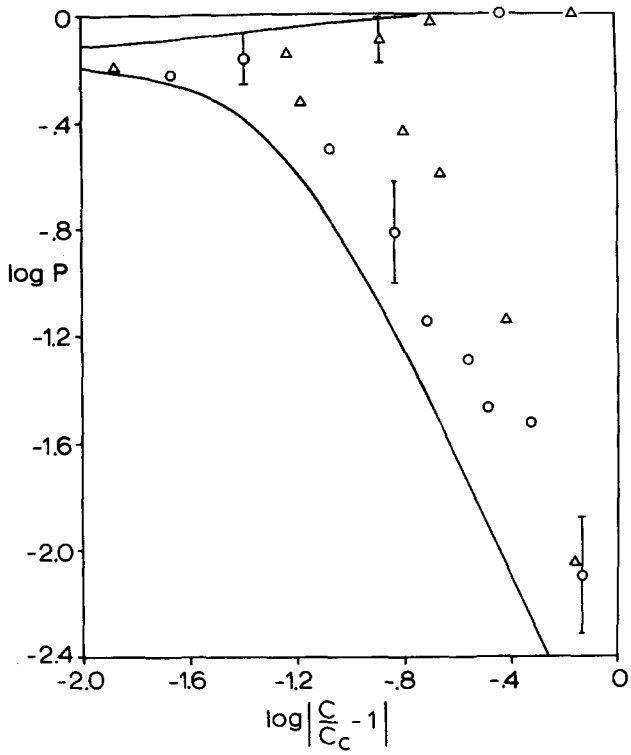

FIG. 5. Percolation critical exponent plot. The line is the theoretical percolation curve for a square lattice assuming a supertrap: guest concentration ratio of 10^{-3}. The critical concentration is $C_c = 0.593$, which gives $P(C = C_c) = 0.649$ in Eq. (3). The experimental points were plotted using this value of $P(C_c) = 0.649$. The corresponding critical concentrations were $C_c = 0.79$ for the 1.8 K data (circles) and $C_c = 0.68$ for the 4.2 K data (triangles). The theoretical line approaches a slope of $-\gamma$ and β as the concentration moves away from C_c to the low or high concentration side, respectively. The 1.8 K data points for $C_g < 0.73$ give $\gamma = 1.6 \pm 0.3$.

give a value as high as 1/3 to 1/2 that of the nearest-neighbor in-plane matrix element.[19,22,23] Moving from two to three-dimensional transfer causes percolation to predict a lower γ value ($\gamma = 1.8$) and a lower C_c value. In this regard, our data is not inconsistent with the percolation theory. A final comment is that we should not lose track of the fact that quasistatic percolation ignores the exciton dynamics, with the exception of the lifetime dependent probability that an exciton will be able to find a supertrap when the two reside on the same maxi-cluster. As we point out in Sec. IIC, ignoring the inter-cluster dynamics is not a bad approximation at very low temperatures and ignoring most of the intracluster dynamics can be both a disadvantage and an advantage. The relationship between static and dynamic percolation has also been discussed by Keyes and Pratt.[30]

Finally, we have compiled the results of several singlet naphthalene experiments reported from this laboratory (Fig. 6). All of the data were taken at superfluid helium temperatures. There are two notable features in this figure. One is the substantial influence of the supertrap concentration on the steady state trapping probability, even with BMN concentrations as high as 0.001. This is consistent with both quasistatic percolation and with diffusion. Figure 6 also compares the steady state trapping probability to that calculated from time resolved measurements for one series of crystals.[24] Parson and Kopelman calculated P using two different procedures. One method consisted of integrating the area under the guest time decay curve $I_g(t)$ relative to the guest decay in a dilute crystal $I_g^0(t)$

$$P = 1 - \frac{\int_0^\infty dt\, I_g(t)}{\int_0^\infty dt\, I_g^0(t)} . \tag{10}$$

The second method used a ratio of measured rate constants, assuming a kinetic model:

$$P = \frac{K_{ET}}{K_{ET} + \tau_g^{-1}} , \tag{11}$$

where K_{ET} is the rate constant for transfer from the guest manifold to a supertrap site and τ_g is the natural lifetime of the naphthalene first excited singlet state. Values of P calculated using Eqs. (10) and (11) were in good agreement with one another. Figure 6 shows that the time resolved trapping probabilities are only in fair agreement, however, with the steady state values reported in this paper. At this time we do not have a reason for this discrepancy other than the inherent differences in the type of experiments as well as the uncertainty in setting $\alpha = 2.0$ in Eq. (9). This discrepancy is not large enough, however, to affect the monotonic dependence of P on C_s observed in Fig. 6.

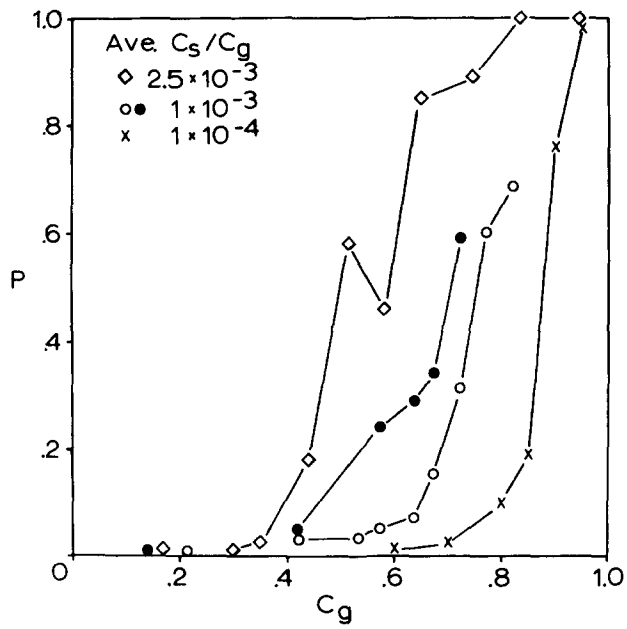

FIG. 6. Trapping probability vs concentration for several experimental studies. The diamonds, open circles, and crosses were all taken from steady state experiments. The open circle data are those presented elsewhere in this paper, with $C_s/C_g = 1 \times 10^{-3}$. The crosses are from Ref. 14 and have $C_s/C_g = 1 \times 10^{-4}$. The diamonds have an average $C_s/C_g = 2.5 \times 10^{-3}$; Ref. 20. The closed circles were taken from time-resolved data using the same crystals as the open circles; Ref. 24. C_s is the BMN concentration and C_g is the $C_{10}H_8$ concentration. All of the data in Fig. 6 were taken at 1.7–1.8 K.

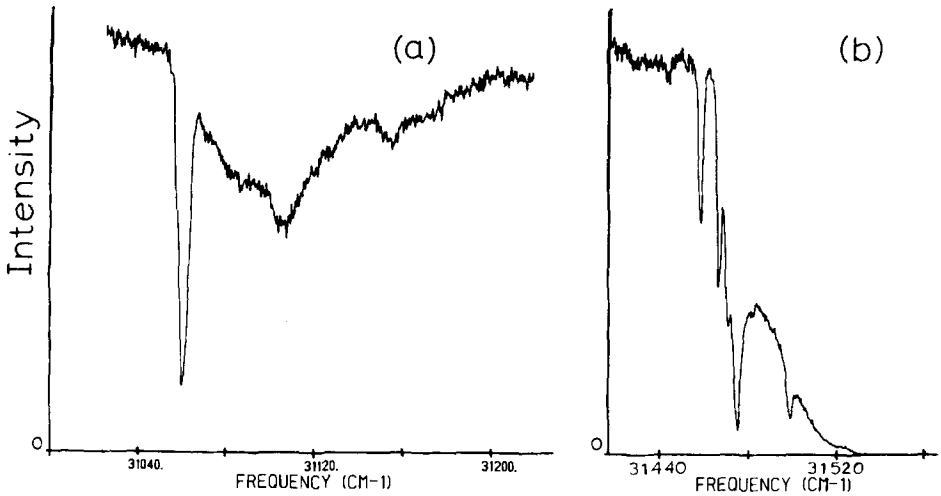

FIG. 7. Absorption spectra of BMN in naphthalene. Fig. 7 (a) is the BMN 0–0 absorption. Fig. 7 (b) is the absorption region near the $C_{10}H_8$ exciton band edge for the same crystal as Fig. 7 (a). The peak at 31 499 cm^{-1} is the 438 cm^{-1} BMN vibronic peak. The peak located at 31 475 cm^{-1} is the $C_{10}H_8$ a Davydov component. The remaining peaks at 31 471, 31 467, and 31 458 cm^{-1} are the 4, 8, and 17 cm^{-1} X traps, respectively.

VI. SUPERTRAP INDUCED ENERGY FUNNEL

A fundamental parameter of any theory which attempts to explain energy transport measured via trapping is the effective trapping radius of the supertrap. Of particular interest is the question of whether energy is funneled to a supertrap site. An example of such an energy funnel is the case where the supertrap molecule perturbs the crystal lattice so as to decrease the excitation energies of the surrounding host and guest molecules. These perturbed sites are similar to the X traps induced by antitrap impurities,[25] except that the molecules perturbed by a supertrap have their luminescence quenched by the supertrap i.e., they are dark X traps. For sake of convenience we will use the term X trap as a generic name to describe any guest or host site whose energy is reduced due to perturbation by an impurity, be it trap *or* antitrap. Presumably the crystal perturbations and the consequent depths of the X traps are largest for the guest and host sites closest to a supertrap. The overall results is that once the exciton lands on a site within the energy funnel (a set of X traps resulting from one supertrap), it has a large probability of energetically cascading down to the supertrap. An extended trapping region of this sort has been claimed for the perdeuteronaphthalene/naphthalene/anthracene crystal system.[26] The question of whether an energy funnel exists for the $C_{10}D_8/C_{10}H_8$/BMN crystal system is relevant to this paper. All three of the theoretical models presented in this paper implicitly assume that the effective trapping radius is approximately limited to the radius of a lattice site.

To test whether the singlet excitons were affected by X traps in our studies, we looked at the optical absorption near the naphthalene band edge. We studied the absorption spectra of 100% $C_{10}H_8$ with and without BMN present as well as 100% $C_{10}D_8$ with and without BMN. Figure 7 shows absorption spectra taken on a 10^{-3} mole fraction BMN/$C_{10}H_8$ crystal. Five peaks are clearly visible in the wavelength range of 3170–3180 Å. Two are easily identifiable. The peak at 31 499 cm^{-1} corresponds to the 438 cm^{-1} BMN vibronic transition. (This is an inband pseudolocalized vibron.) The low energy $C_{10}H_8$ Davydov component is located at 31 475 cm^{-1}. The remaining peaks located at 4, 8, and 17 cm^{-1} to the low energy side of the naphthalene Davydov peak are visible only when BMN is present in the crystal. We have attributed these peaks to BMN induced X traps. We can rule out X traps induced by other impurities in the BMN stock mixture: the 17 cm^{-1} trap should be deep enough at 1.8 K to lead to X trap emission unless the exciton is passed on to an even deeper trap, i.e., BMN.

Interpreting the 4, 8, and 17 cm^{-1} red shifted peaks as BMN induced X traps provides us with some insight into the trapping process. There may be a large number of naphthalene molecules with excitation energies slightly perturbed by a given supertrap site. It is only those molecules whose energies lie outside of the $C_{10}H_8$ exciton band, however, which will significantly affect energy transfer. The extinction coefficient for the naphthalene X traps should be equal to or larger than the coefficient for BMN. This is based on experiments in the literature concerning various isotopic naphthalene dopants in naphthalene as well as on the theoretically predicted Rashba effect.[27,28] We used this fact along with our absorption spectra to calculate that the total number of X traps below the guest band must be about equal to or less than the number of BMN sites. There should not be a significant change in the influence of these X traps when going from a 100% $C_{10}H_8$ crystal to the isotopically mixed crystals. The guest bandwidth does not change much above the critical concentration[27] and below the critical concentration an energy funnel will have little effect on the energy transport.

We can speculate as to the nature of the BMN X-trap structure in the absorption spectrum. Theoretically there are two inequivalent orientations for a monosubstituted naphthalene placed on a given site in an otherwise pure naphthalene crystal. This orientation splitting is visible with 1-$D_1C_{10}H_7$ in $C_{10}D_8$,[28] but is not visible with BMN in either $C_{10}H_8$ or $C_{10}D_8$. Consequently, BMN most likely has a preferred orientation in the ground state. The presence of the methyl substituent breaks down the crystal symmetry, thus uniquely defining all of the neighboring lattice sites, e.g., the four nearest neighbors will all differ from one another in their distances from the $-CH_3$ group. Although a com-

plete elucidation requires accurate force field and quantum mechanical calculations, it is reasonable to expect that those individual sites closest to the methyl substituent would experience the largest perturbation.

It is quite difficult to calculate an exact number of X-trap sites since the uncertainties in the absorbance and the extinction coefficients are sizable. It is possible tp conclude, however, that an energy funnel cannot extend beyond the nearest neighbors of the supertrap. Consequently, using the percolation and diffusion models to explain our experimental results is justified with respect to the criterion of the absence of large energy funnels in this system.

VII. SUMMARY AND CONCLUSIONS

The experimental results reported in this paper offer an improvement in the quality of information available on singlet exciton transport in substitutionally disordered naphthalene. This increase in quality is due to advances in instrumentation as well as the accumulation of experience in this laboratory. The data allows us to reach some general conclusions regarding the applicability of existing transport theories.

(1) Generalized diffusion models such as those suggested by GAF and by Blumen and Silbey, assuming octupole–octupole transfer, offer good agreement with our experimental data at 4.2 K. At this temperature, medium or long range transfer is no longer negligible. Fitting the theoretical curve to the data, however, does require a physically questionable value of 8 Å for the adjustable interaction parameter R_0.

(2) At 1.8 K the diffusion models are no longer consistent with our experimental data, assuming the same octupole–octupole transfer interactions as for the 4.2 K data. The cause for this breakdown can be attributed to the energetic differences between the nearest-neighbor clusters and/or the inapplicability of treating the excitons as localized states. At this temperature the data is consistent with percolation, provided that we replace the static model with the quasistatic model. A weakness of these percolation models is that the dynamical nature of exciton transport is ignored, with the exception of a model dependent adjustable parameter for quasistatic percolation, e.g., a random walk coherence length.

(3) There is no significant enhancement in the trapping probability due to large energy funnels. The size of the BMN lattice distortions is such that no molecules beyond the immediate neighbor guest sites have excitation energies shifted lower than the guest band edge.

(4) Experimental studies of the type discussed in this paper should not treat the ratio of phonon sideband emission intensity relative to zero-phonon intensity as a constant with respect to optical polarization or crystal concentration, as is usually done. There is a significant breakdown in the Condon approximation leading to a Herzberg–Teller type coupling of the lattice vibrations to the vibronic transitions.

This paper has made no attempt to test one generalized diffusion model relative to another. Their predictions are practically identical within experimental error. Further studies of the transport phenomenon will need to be based on fast and accurate time resolved measurements. Steady state experiments, however, provide us with a general overview of the applicability of various approaches to exciton transport in mixed molecular crystals.

ACKNOWLEDGMENTS

We would like to thank Robert Parson for many fruitful theoretical discussions. We also thank R. F. Loring and M. D. Fayer for sending us a preprint of their work as well as for several private communications.

[1](a) A. S. Davydov, Eksp. Teor. Fiz. **18**, 210 (1948); (b) *Theory of Molecular Excitations* (McGraw–Hill, New York, 1962); (c) D. P. Craig and S. H. Walmsley, *Excitons in Molecular Crystals: Theory and Applications* (Benjamin, New York, 1968); (d) R. Silbery, Annu. Rev. Phys. Chem. **27**, 203 (1976); (e) C. B. Harris and D. A. Zwemer, *ibid.* **29**, 473 (1978); (f) D. Burland and A. Zewail, Adv. Chem. Phys. **50**, 385 (1980); (g) H. C. Wolf and H. Port, J. Lumin. **12/13**, 33 (1976); (h) V. L. Broude, E. Rashba, and E. F. Sheka, *Spectroscopy of Molecular Excitons* (Energozdat, Moscow, 1981); (i) R. C. Powell and Z. G. Soos, J. Lumin. **11**, 1 (1975); (j) V. M. Kenkre and R. S. Knox, Phys. Rev. B **9**, 5279 (1974).

[2]R. Kopelman, in *Radiationless Processes in Molecules and Condensed Phases, Topics in Applied Physics*, edited by F. K. Fong (Springer, Berlin, 1976), Vol. 15, p. 297.

[3]A. H. Francis and R. Kopelman, in *Laser Spectroscopy of Solids, Topics in Applied Physics*, edited by W. M. Yen and P. M. Selzer (Springer, Berlin, 1981), Vol. 49, p. 241.

[4]K. Godzik and J. Jortner, J. Chem. Phys. **72**, 4471 (1980).

[5]R. F. Loring and M. D. Fayer, Chem. Phys. **70**, 139 (1982).

[6](a) C. R. Gochanour, H. C. Andersen, and M. D. Fayer, J. Chem. Phys. **70**, 4254 (1979); (b) R. F. Loring, H. C. Andersen, and M. D. Fayer, *ibid.* **76**, 2015 (1982).

[7]A. Blumen and R. Silbey, J. Chem. Phys. **70**, 3707 (1979).

[8]S. W. Haan and R. Zwanzig, J. Chem. Phys. **68**, 1879 (1978).

[9]A. Blumen and J. Manz, J. Chem. Phys. **71**, 4694 (1979).

[10]S. R. Broadbent and J. M. Hammersley, Proc. Cambridge Philos. Soc. **53**, 629 (1957).

[11]S. D. Colson, S. M. George, T. Keyes, and V. Vaida, J. Chem. Phys. **67**, 4941 (1977).

[12](a) D. M. Hanson, J. Chem. Phys. **52**, 3409 (1970); (b) J. Hoshen and R. Kopelman, Phys. Status Solidi B **81**, 479 (1977); (c) E. Monberg, Ph.D. thesis, University of Michigan, 1977; (d) H. K. Hong and R. Kopelman, J. Chem. Phys. **57**, 3888 (1972); (e) R. LeSar and R. Kopelman, Chem. Phys. **29**, 289 (1978); (f) Ph. Pee, R. Lalanne, F. Dupuy, and Ph. Kottis, *ibid.* **28**, 407 (1978); (g) K. E. Mauser, H. Port, and H. C. Wolf, *ibid.* **1**, 1 (1973).

[13]D. C. Ahlgren and R. Kopelman, Chem. Phys. Lett. **77**, 135 (1981).

[14]P. Argyrakis and R. Kopelman, Chem. Phys. **57**, 29 (1981).

[15](a) J. Hoshen and R. Kopelman, J. Chem. Phys. **65**, 2817 (1976); (b) J. Hoshen, R. Kopelman, and E. M. Monberg, J. Stat. Phys. **19**, 219 (1978).

[16]J. Newhouse, R. Kopelman, and J. Hoshen (unpublished).

[17]E. M. Monberg and R. Kopelman, Mol. Cryst. Liq. Cryst. **57**, 271 (1980).

[18](a) M. Köhler, D. Schmid, and H. C. Wolf, J. Lumin. **14**,

41 (1976); (b) A. Pröpstl and H. C. Wolf, Z. Naturforsch. Teil A **18**, 822 (1963); (c) R. C. Powell and Z. G. Soos, J. Lumin. **11**, 1 (1975).
[19]J. B. W. Morsink and D. A. Wiersma, Chem. Phys. Lett. **89**, 291 (1982).
[20]R. Kopelman, E. M. Monberg, and F. W. Ochs, Chem. Phys. **21**, 373 (1977).
[21](a) R. Kopelman, F. W. Ochs, and P. N. Prasad, J. Chem. Phys. **57**, 5409 (1972); (b) F. W. Ochs, P. N. Prasad, and R. Kopelman, Chem. Phys. Lett. **29**, 290 (1974); (c) K. P. Meletov and E. F. Sheka, Mol. Cryst. Liq. Cryst. **43**, 203 (1977); (d) S. D. Colson, T. L. Netzel, and J. M. van Pruyssen, J. Chem. Phys. **62**, 606 (1975).
[22]H. K. Hong and R. Kopelman, J. Chem. Phys. **57**, 3888 (1972).
[23]F. W. Ochs and R. Kopelman, J. Chem. Phys. **66**, 1599 (1977).
[24]R. P. Parson and R. Kopelman, Chem. Phys. Lett. **87**, 528 (1982).
[25]H. C. Wolf and K. W. Benz, Pure Appl. Chem. **27**, 439 (1971).
[26](a) Z. G. Soos and R. C. Powell, Phys. Rev. B **6**, 4035 (1972); (b) H. Auwetter, A. Braun, U. Mayer, and D. Schmid, Z. Naturforsh. Teil A **34**, 761 (1979).
[27]R. Kopelman, in *Excited States II*, edited by E. C. Lim, (Academic, New York, 1975).
[28]F. W. Ochs, P. N. Prasad, and R. Kopelman, Chem. Phys. **6**, 253 (1974).
[29]J. Hoshen and R. Kopelman, Phys. Rev. B **14**, 3438 (1976).
[30]T. Keyes and S. Pratt, Chem. Phys. Lett. **65**, 100 (1979).